

Oxidative Stress and Plasma Membrane Repair in Single Myoblasts After Femtosecond Laser Photoporation

XINXING DUAN,^{1,3} KAM TAI CHAN,^{1,2} KENNETH K. H. LEE,^{1,4} and ARTHUR F. T. MAK^{1,2,3}

¹Division of Biomedical Engineering, The Chinese University of Hong Kong, Shatin, Hong Kong

²Department of Electronic Engineering, The Chinese University of Hong Kong, Shatin, Hong Kong

³Department of Mechanical and Automation Engineering, The Chinese University of Hong Kong, Shatin, Hong Kong; and ⁴School of Biomedical Sciences, The Chinese University of Hong Kong, Shatin, Hong Kong

(Received 30 December 2014; accepted 14 May 2015; published online 27 May 2015)

Associate Editor James Tunnell oversaw the review of this article.

Abstract—Cell membranes are susceptible to biophysical damages. These biophysical damages often present themselves in challenging oxidative environments, such as in chronic inflammation. Here we report the damage evolution after single myoblasts were individually subjected to femtosecond (fs) laser photoporation on their plasma membranes under normal and oxidative conditions. A well-characterized tunable fs laser was coupled with a laser scanning confocal microscope. The post-damage wound evolution was documented by real-time imaging. The fs laser could generate a highly focused hole at a targeted site of the myoblast plasma membrane. The initial hole size depended on the laser dosage in terms of power and exposure duration. With the same laser power and irradiation duration, photoporation invoked bigger holes in the oxidative groups than in the control. Myoblasts showed difficulty in repairing holes with initial size beyond certain threshold. Within the threshold, holes could apparently be resealed within 100 s under the normal condition; while in oxidative condition, the resealing process could take 100–300 s. The hole-resealing capacity of myoblasts was compromised under oxidative stress particularly when the oxidative exposure was chronic. It is interesting to note that brief exposure to oxidative stress apparently could promote resealing in myoblasts after photoporation.

Keywords—Femtosecond laser photoporation, Plasma membrane damage, Damage evolution and repair, Oxidative stress.

INTRODUCTION

Plasma membrane damage is common for cells in load bearing tissues such as skeletal and cardiac muscles, which are constantly exposed to biophysical stresses.^{2,18} In the normal condition and when the damages are within certain threshold, cells can repair their plasma membrane damage.^{19,24} To repair plasma membrane disruptions in a timely manner, cells initiate a membrane patching process to rapidly reseal the membrane breach.^{24,27} The cytoskeleton is reorganized to facilitate the repair process.^{5,16} While the molecular responses to cellular damages have been well studied, such as the engagements of annexin,¹⁷ MG53,⁷ Rho family GTPases,⁵ E-cadherin¹ and so on, the biophysical processes of damage development and damage repair have been reported relatively less.

Oxidative stress is a physiological condition when the reactive oxygen species generated exceed the coping capacity of cells. Oxidative stress are reportedly associated with many pathological conditions, such as inflammation,⁶ muscle atrophy,²¹ cancer,¹² Alzheimer's diseases⁴ *etc.* To cope with oxidative stress, genes for specific enzymes and proteins that serve protective functions are up-regulated; while others are down-regulated to conserve energy.^{9,13} Our group has recently reported that oxidative stress could affect myoblast stiffness *via* the RhoA signaling pathways,²⁵ and the cytoskeletal actin polymerization in myotubes *via* regulatory proteins cofilin and thymosin-beta-4.²⁸ We hypothesized here that oxidative stress may make cells more vulnerable to biophysical damages and adversely affect the subsequent repair process. This hypothesis was supported by our recent findings that

Address correspondence to Arthur F. T. Mak, Division of Biomedical Engineering, The Chinese University of Hong Kong, Shatin, Hong Kong. Electronic mail: arthurmak@cuhk.edu.hk

oxidative stress could affect the damage thresholds of myoblasts in monolayer subjected to a spatially varying compressive stress field under indentation.²⁹ In this paper, we aimed to study how oxidative stress may affect the damage-repair kinetics of single myoblasts by individually perforating single site on plasma membrane.

Many approaches have been developed to perforate plasma membrane for drug/gene delivery and other biomedical applications, including micropipette manipulation,^{8,26} electroporation,^{10,22} and ultrasound sonoporation.^{12,15,30} However, micropipette manipulation requires sophisticated skills, lacks a reliable measurement of damage dosage, and thus does not facilitate a precise and repeatable control for studying single cell damage. Electroporation and sonoporation, on the other hand, can provide quantitative damage dosage on many cells, but are not able to target damage at a specific site on single cells. Among all the perforation techniques, femtosecond laser, known for minimum collateral damage due to its ultrashort pulses, can be used as a site-specific, non-contact, controllable and quantifiable method with high temporal and spatial accuracy.^{3,11} In this study, we applied femtosecond laser photoporation as the damage method to disrupt a highly specific membrane site with precise control of damage dosage.

Our overall hypotheses for this study were as follows. First, cell wound would vary in size with different fs laser dosages. Second, cell damage-repair evolution would differ if the cell is exposed to an oxidative environment.

MATERIALS AND METHODS

Laser Setup

A Ti: Sapphire mode-locked fs laser (MaiTai HP, Spectrum Physics Inc.) was coupled with a fluorescent laser scanning confocal microscopy system (TCS SP5, Leica Microsystems) as the experimental platform (Fig. 1). The fs laser was able to target the highly-focused single-site damage on the plasma membrane of selected cells. The confocal microscope was used to acquire real-time live images of wound evolution process after fs laser photoporation.

In our experiment, the wavelength of the MaiTai HP fs laser (output wavelength range 690–1020 nm, repetition rate 80 MHz) was set at 800 nm. It could generate 100 fs laser pulses with an average power range of 40–120 mW at 800 nm. The pulsed laser beam was directed into the confocal microscope light path and tightly focused to a femtolitre focal volume at the basal plasma membrane by a 63× water immersion objective with a numerical aperture (*NA*) of 1.2. With

this femtosecond laser apparatus, a focal perforation could be generated on the plasma membrane of a single cell. Argon laser at 488 nm and He–Ne laser at 633 nm were both applied in the experiment to excite the fluorescent staining of the cells.

Cell Sample Preparation

Cell Culture

C₂C₁₂ myoblasts (#CRL-1772, ATCC Organization) were seeded in 35 mm confocal dish (SPL Lifesciences Inc.) at a density of 50,000 cells per dish. Dulbecco's modified Eagle medium (DMEM, gibco®, Life Technologies Inc.) supplemented with 10% Fetal Bovine Serum (FBS, gibco®, Life Technologies Inc.) and 1% Penicillin streptomycin (Pen Strep, gibco®, Life Technologies Inc.) was used as the culture medium. The sample dishes were then placed in an incubator at 37 °C temperature and with 5% carbon dioxide for 48 h to foster cell attachment and proliferation.

H₂O₂ Treatment

Hydrogen peroxide (H₂O₂, Unichem Inc.) was employed as an extrinsic oxidant in the experiment to impose oxidative stress on the myoblasts. In this study, two different concentrations of H₂O₂ were applied to the cells—2 and 0.5 mM.^{23,25} To study the chronic and acute effects of the imposed oxidative stress, two treatment duration were chosen—1 and 24 h. More than 90% cells showed signs of being severely insulted when myoblasts were treated with 2 mM H₂O₂ for 24 h. Thus 2 mM H₂O₂ treatment was only used in the 1 h acute oxidative study. In all, we have 3 groups of oxidative stressed C₂C₁₂ myoblast cells—0.5 mM H₂O₂ for 1 h, 0.5 mM H₂O₂ for 24 h and 2 mM H₂O₂ for 1 h.

For acute H₂O₂ treatment groups (0.5, 2 mM/1 h), the C₂C₁₂ cells were first seeded in a confocal dish and incubated for about 46 h. The cells were taken out from the incubator and the culture medium was then replaced by the 0.5/2 mM oxidative medium. The cells were put back into the incubator for 1 h. After that, the cells were taken out of the incubator and rinsed with PBS for 3 times. The H₂O₂ treated cells were then ready for staining.

For the chronic H₂O₂ treatment group (0.5 mM/24 h), the cell culture medium was replaced by the oxidative medium after only 24 h incubation of the seeded cells and the oxidative treatment lasted for another 24 h, all in a 37 °C and 5% carbon dioxide incubation environment. After that, the cells were taken out of the incubator and rinsed with PBS for 3 times before staining.

Cell Staining Method

All the cells were first stained with calcein AM (excitation/emission maxima: 488/536 nm Molecular Probes[®], Life Technologies Inc.) at a concentration of 1 $\mu\text{g}/\text{mL}$ for signaling cell viability. After 10 more minutes of incubation, the medium was removed and the cells were washed 3 times using PBS. The cells were then stained with a plasma membrane dye (excitation/emission maxima: 650/680 nm, CellMask, Molecular Probes[®], Life Technologies Inc.) at a concentration of 5 $\mu\text{g}/\text{mL}$ and incubated for another 10 min. Likewise, after incubation, the medium was removed and the cells were washed 3 times. Fresh culture medium was then added into the sample dish. The cells sample was ready for the laser photoporation experiment.

Fs Laser Operation and Imaging Protocol

Power Measure and Calibration

In this study, the fs laser was set at 3 average powers, namely 55/80/110 mW to deliver photoporation damage on the plasma membrane. The laser power was first calibrated as follows.

A slide power meter (Thorlabs Co Ltd.) was employed to measure the average power irradiated on the sample. As shown in Fig. 1, the power meter was placed at the same position as the cells sample. The MaiTai HP fs laser control system was integrated with the confocal microscopic control software (Leica LAS AF). The power of the fs laser was tuned in the LAS AF software system. A 10-s fs laser irradiation was executed for testing. The average irradiation power was measured by the power meter. The testing procedures were repeated several times and every time the laser power was adjusted until the specific average power (e.g., 55 mW) was attained. Then the laser power was fixed in the control software and testing was conducted for another 3 times to assure the average power is stable. Once the laser power was found stable at the target power, the fs laser was ready for plasma membrane photoporation experiment.

The laser average power was calibrated once every 2 h during the experiment just in case the fs laser power drifted from the desired settings.

Fs Laser Irradiation Protocol

After the fs laser was calibrated at the target power, the power meter was removed from the stage and the cells sample was placed on the stage instead. A living cell with calcein staining was selected and identified under the confocal microscope. The fs laser was then focused at a specific site on the basal plasma membrane of the cell. The fs laser irradiation site was a

roughly round spot with an aspect ratio of 0.9–1.1. The diameter of the fs laser light spot could be estimated by Rayleigh's Criterion:

$$d = \frac{0.61\lambda}{NA} \quad (1)$$

where λ is the wavelength of the fs laser light, NA is the numerical aperture of the objective. In this study, the diameter of the light spot was estimated roughly at 407 nm. The depth of the spot could be estimated by the axial resolution of the confocal microscope at fs laser wavelength, which is usually given as:

$$R_{\text{axial}} = \frac{0.88\lambda}{n - \sqrt{n^2 - (NA)^2}} \quad (2)$$

where λ is the wavelength of the illuminating light (for calculating depth of fs laser spot 800 nm), n is the refractive index of the immersion medium (1.33), NA is the objective numerical aperture (1.2).²⁰ Thus, the depth of the fs laser spot was estimated to be 931 nm.

The criteria of choosing the fs laser irradiation site were as follows:

- (a) on the basal plasma membrane;
- (b) generally along the long axis of the cell;
- (c) preferentially on the side with a larger membrane area;
- (d) roughly at the midpoint between the cell boundary and the nucleus envelope.

The fs laser irradiation time was set as 2 ms in all the experiments in this study.

After a cell was irradiated by the fs laser at a specific point on the basal plasma membrane, an elliptical hole emerged at the irradiation site of the cell.

Imaging Protocol

A specific region for image was manually selected in the microscopic imaging suite (LAS AF software, Leica Microsystems) to narrow down the image field to a single cell size. Then a 3D volume fluorescent scanning of the cell was taken ($\sim 0.5 \mu\text{m}$ per layer) at the speed of 1.3 s per frame before fs laser irradiation. The scanning image size of each layer was 512×512 pixel. Following the 2 ms fs laser irradiation, a sequence of 2D time-lapse images at a time interval of 5.2 s were acquired immediately. This real-time post-damage observation lasted up to 5–7 min.

Data Analysis

The hole size was calculated by a self-developed MATLAB programme (Version 2012, the Mathworks

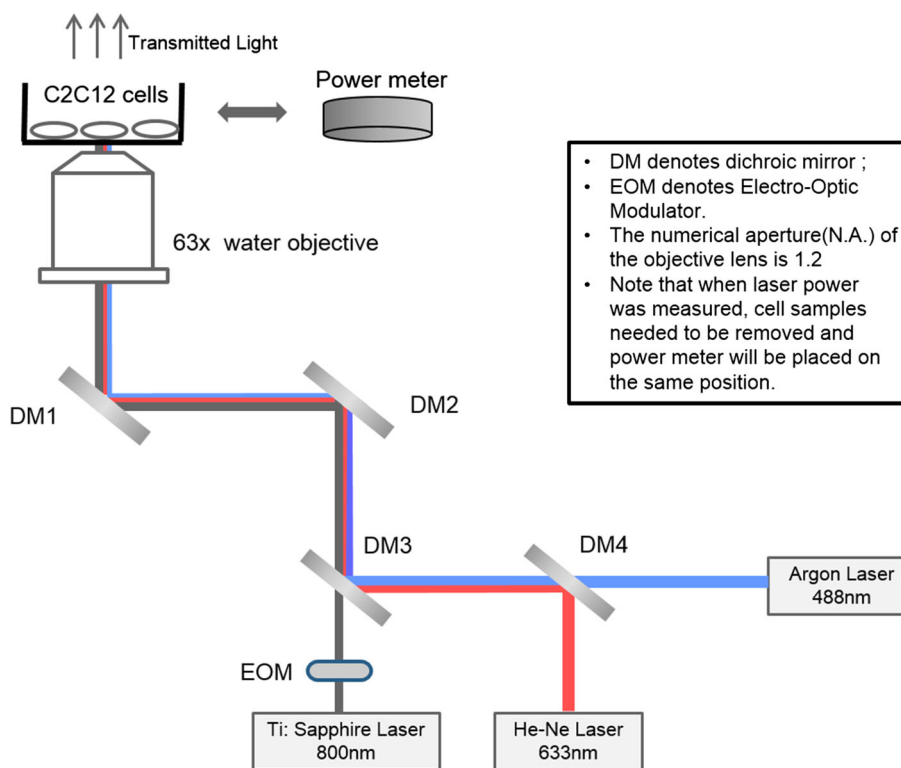


FIGURE 1. The schematic of the experimental setup.

Inc.). Feature comparisons among different groups were processed by the GraphPad Prism software (Version 5, GraphPad Software Inc.) based on the Student's *t* test. Data correlations were studied by the Pearson product-moment correlation coefficient (Pearson's *r*). Sample size was determined by the statistical power analysis.

RESULTS

Scenarios of Damage Evolution

Four scenarios of damage evolution were found after single cell fs laser photoporation in all.

- (i) The fs laser-induced hole was gradually resealed within the 5 min observation. An example was shown in Fig. 2.
- (ii) The fs laser-induced hole became smaller but not fully resealed (Fig. 3).
- (iii) The cell was split and fell apart after fs laser photoporation (Fig. 4).
- (iv) The post-damage wound dynamics had two phases—resealed and re-split. In the first phase, the initial laser-induced hole was resealed. In the second phase, another hole

close to the site of the initial hole emerged and expanded (Fig. 5).

Scenarios (i) and (ii) were most frequently observed. The two scenarios accounted for ~95% among all the cells after photoporation by 55/80/110 mW for 2 ms. Scenarios (iii) and (iv) were much less common. This showed that the cells generally launched a resealing response to the laser photoporation. This resealing process could be a reasonable indicator of the self-repair ability of a cell.

Initial Hole Size (IHS)

The initial wound size of the plasma membrane varied with the dosage of fs laser irradiation. With 2 ms fs laser irradiation, the higher the laser power, the bigger the wound would be. As shown in Fig. 6a, the average hole size for 55 mW irradiation was $3.7 \mu\text{m}^2$, which was smallest in the three groups. The group of 80 mW showed a larger average hole size of $7.0 \mu\text{m}^2$. The 110 mW group showed the biggest average hole area of $14.8 \mu\text{m}^2$. The hole size was positively correlated with the laser power (correlation coefficient $r = 0.984$), suggesting that the initial hole size could be taken to reflect the damage level of the fs laser irradiation.

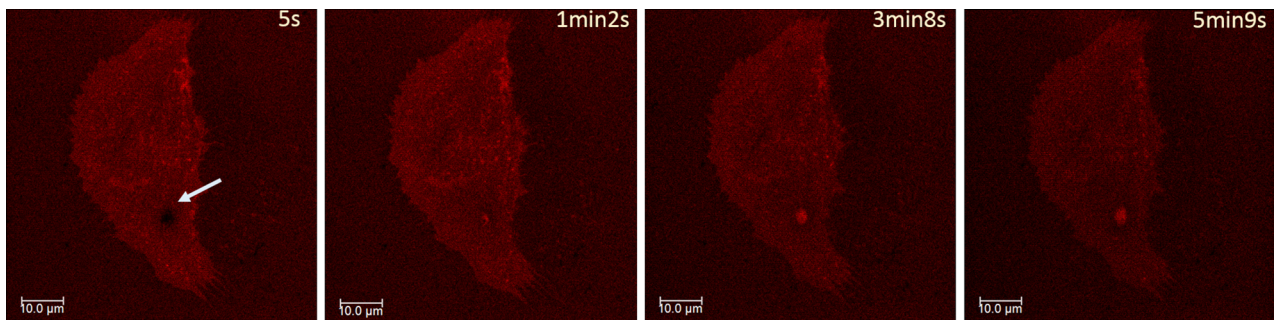


FIGURE 2. Wound dynamics: the fs laser-induced hole was fully resealed. The cell was damaged by 55 mW laser for 2 ms. The white arrow pointed to the initial hole.

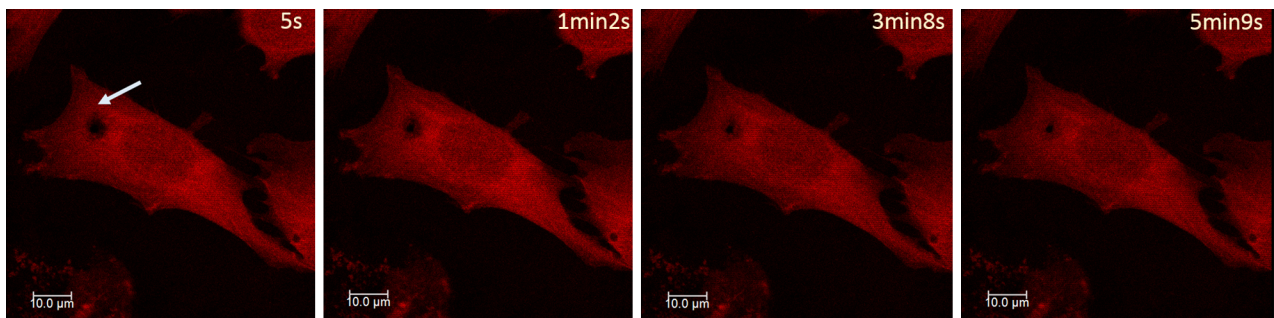


FIGURE 3. Wound dynamics: the fs laser-induced hole became smaller but not fully resealed after 5 min. The cell was damaged by 110 mW laser for 2 ms. The white arrow pointed to the initial hole.

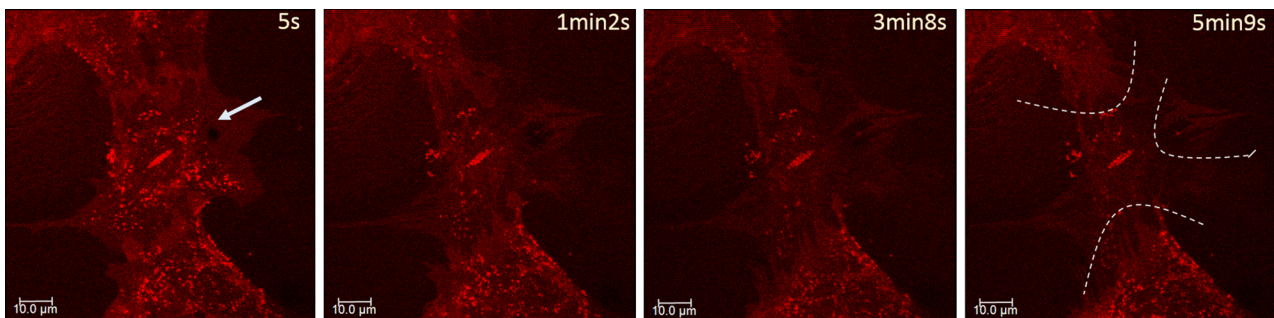


FIGURE 4. Wound dynamics of a split cell after photoporation by 80 mW laser for 2 ms. The white arrow pointed to the initial hole. The dashed white line showed the split parts of the cell.

IHS in the oxidative stress groups showed striking differences compared to the control groups (Fig. 6b). The average hole sizes in the 0.5 mM/24 h H₂O₂ group (6.6 μm²) were significantly larger than those in the 0.5 and 2 mM/1 h groups. The average hole sizes in the 2 mM/1 h group (5.5 μm²) was slightly larger than that of the 0.5 mM/1 h group (5.4 μm²), but there was no significant difference between the two groups. These results supported that chronic oxidative stress could make plasma membrane more vulnerable to biophysical damage than acute oxidative stress.

Resealing Ratio

The resealing results varied. Some cells were capable of fully resealing the wound induced by photoporation, while some could only partly reseal the wound. The hole size data showed that whether a cell could reseal a photoporated wound depended on the initial hole size. As shown in Fig. 7a, for the holes with size below 5 μm², the resealing ratio (the ratio of the number of the cells with their wounds resealed to the total number of photoporated cells) was up to 100% (including one re-split cell), while only 25% of the photoporated cells

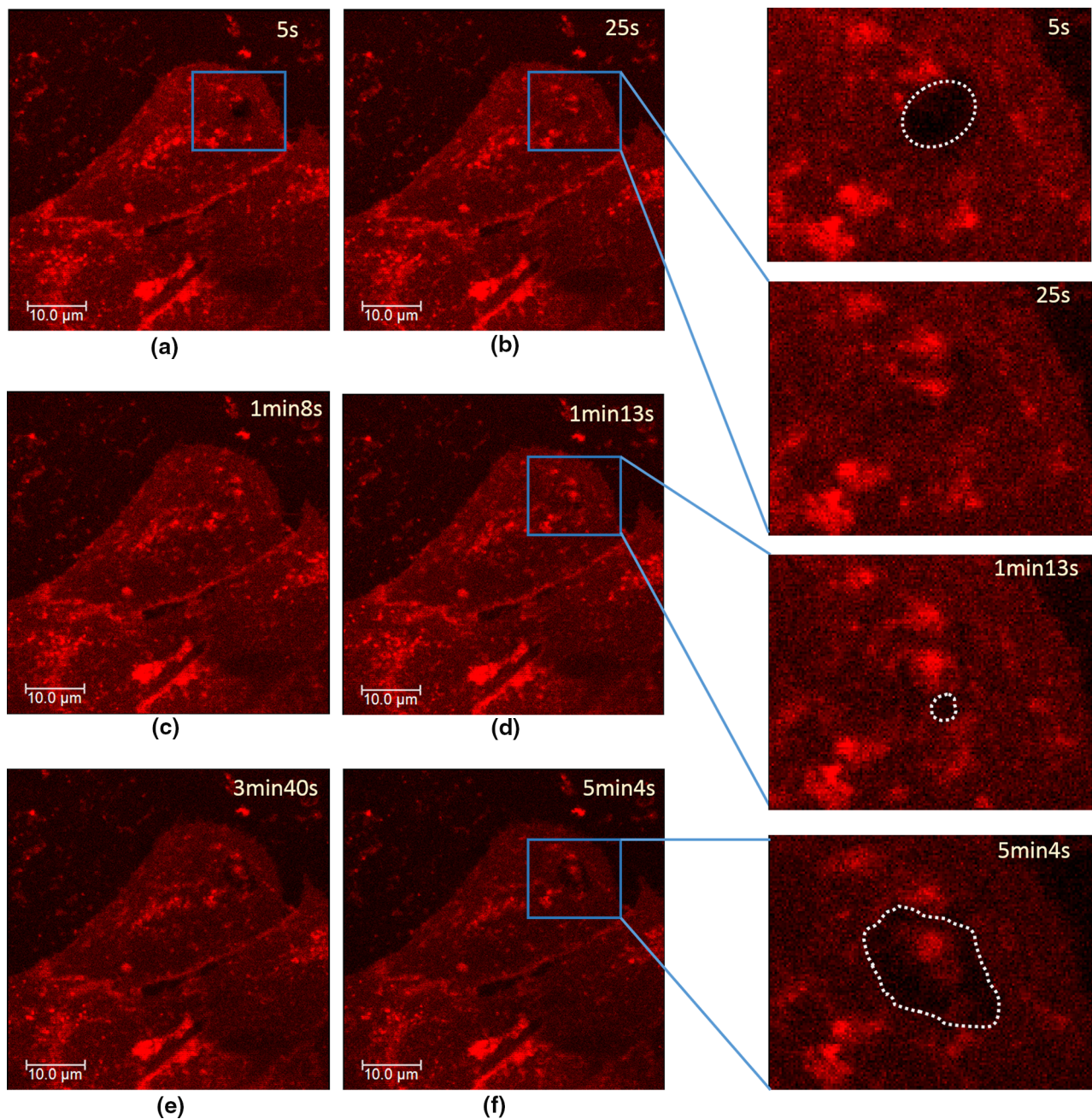


FIGURE 5. The resealing and re-splitting wound dynamics of a cell. (a, b, c) The initial hole resealing phase; (d, e, f) The re-split phase. (a) The initial hole was induced by 55 mW/2 ms laser. (b) The initial hole was resealed ~25 s after laser irradiation. (c) The plasma membrane remained intact at ~68 s. (d) A new hole emerged ~73 s after laser irradiation. (e, f) The newly emerged hole expanded. The white dashed lines circled the holes on the plasma membrane. The blue rectangles denoted the zoom area of hole size.

had the ability to reseal holes with size above $5 \mu\text{m}^2$. The significant difference indicated that the cells had difficulty coping with bigger holes.

Apparently, the cells showed good hole-repair ability (resealing ratio 100%) if the hole was smaller than $5 \mu\text{m}^2$. Thus holes smaller than $5 \mu\text{m}^2$ are within the safe range of repair. For holes bigger than $10 \mu\text{m}^2$, the damage was beyond the self-repair ability

of the cells and all the holes remained unsealed. For the interim range with hole size from 5 to $10 \mu\text{m}^2$, only some of the cells could repair themselves (~44%). Based on this observation, three damage ranges are partitioned according to the initial hole size: safe range, $\text{IHS} < 5 \mu\text{m}^2$; interim range, $5 \mu\text{m}^2 < \text{IHS} < 10 \mu\text{m}^2$; fatal range, $\text{IHS} > 10 \mu\text{m}^2$ (see Fig. 7a).

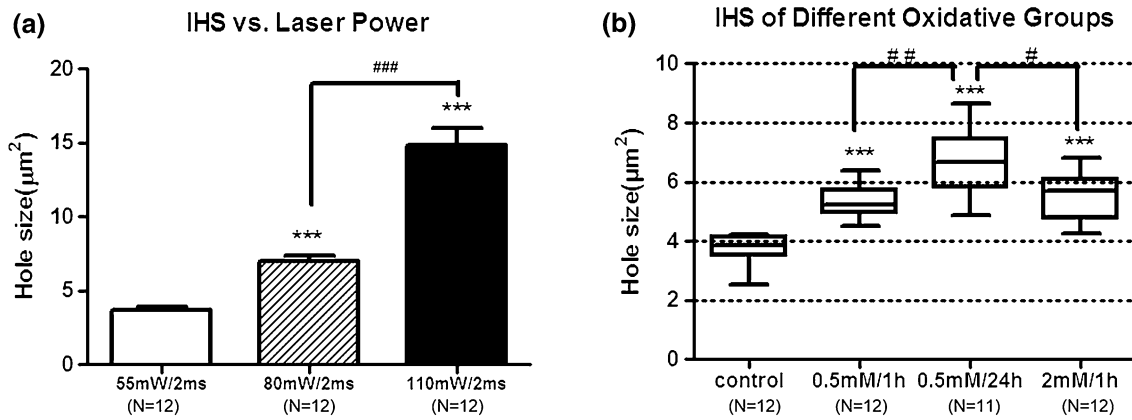


FIGURE 6. IHS in different groups. (a) Comparison of the IHS with different laser power levels. IHS of 80 and 110 mW groups were both significantly larger than that of the 55 mW groups. IHS of the 80 and 110 mW groups were also significantly different. (b) The Box-and-Whisker Plots of IHS of the control groups and the three H₂O₂ treatment groups (laser: 55 mW/2 ms). All of the three H₂O₂ groups showed significantly larger holes compared to the control group. (***) $p < 0.001$; ### $p < 0.001$; # $p < 0.01$; # $p < 0.05$.

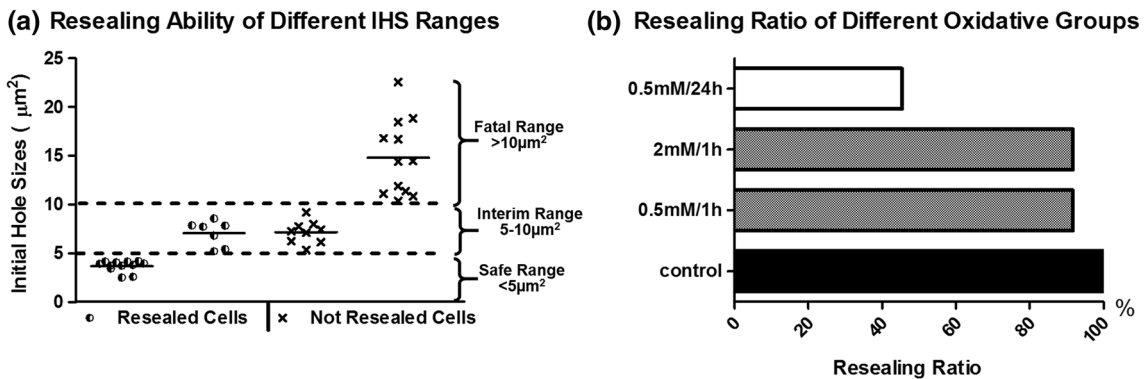


FIGURE 7. Cell resealing ability comparisons. (a) The IHS and resealing results of individual cells after photoporation by 55/80/110 mW laser for 2 ms, showing the mean and range of IHS of each group. (b) The resealing ratio of the control groups and the three H₂O₂ treatment groups after single cells were photoporated by 55 mW laser for 2 ms.

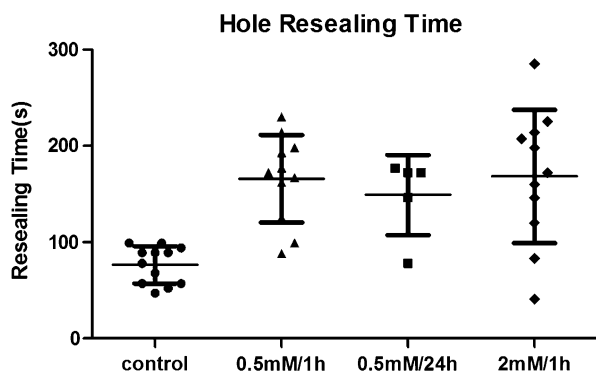


FIGURE 8. The scatter plots of the hole resealing time of the control groups and the three H₂O₂ treatment groups, showing the mean and standard deviation of each group. All cells were irradiated by 55 mW/2 ms fs laser.

Resealing ratio of the three oxidative groups were calculated and compared to that of the control group. As shows in Fig. 7b, while the resealing ratio in the

control group was high up to 100%, the 0.5 mM/24 h H₂O₂ group showed a much lower resealing ratio at 45.5%. This indicated that long exposure of oxidative stress significantly compromised the self-repair capacity of myoblasts for biophysical damage on the plasma membrane. On the other hand, both the 0.5 and 2 mM/1 h H₂O₂ groups kept a relatively high resealing ratio above 90%.

Resealing Time

In normal condition, the hole resealing was a fast process. Hole resealing time was estimated according to the hole size analysis of an image at a specific time. When the estimated hole size became smaller than a pixel and the hole disappeared in the acquired image, the image capture time was defined as the hole resealing time. All the cells that have successfully resealed the hole could complete the resealing process within 300 s. Among them, over 90% of the resealed

Resealing Ratio of Cells with Interim Range IHS

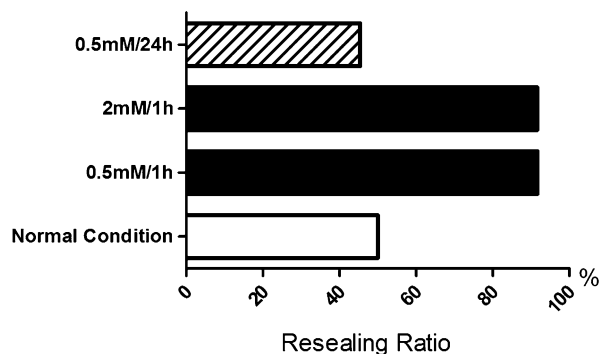


FIGURE 9. The resealing ratios of the cells with hole size in the interim range in normal and oxidative conditions. The oxidative groups were irradiated by 55 mW/2 ms fs laser, and the normal group was irradiated by 80 mW/2 ms fs laser to obtain the interim range IHS in their specific conditions.

cells had the hole resealed within 100 s. (The analysis was based on the resealed cells of all 55, 80 and 110 mW laser insult groups.)

The time to reseat the hole induced by 55 mW/2 ms fs laser was measured in the three oxidative groups (Fig. 8). The resealed holes in the control group were all resealed within 100 s. Compared to the control group, the holes in the H₂O₂ treated groups resealed much slower. The resealing time was mostly between 100 and 300 s. There were no clear differences in the resealing time among the three oxidative groups.

DISCUSSION

Wound Evolution Features in Normal Conditions

From the scenarios of wound evolution, the wound of most cells (>90%) became smaller within the 5 min of post-damage observation. This indicated that cells generally launched a resealing process after fs laser photoporation. However, not all the resealing process could lead to complete wound closure. The resealing result was probably dependent on the IHS. This observation was consistent with the downstream repair process of cells after sonoporation.¹⁴ Cells could more likely close their wounds when the initial wound size was smaller. The safe range was suggested to be with IHS below 5 μm^2 , and the fatal range was suggested to be above 10 μm^2 . IHS was also directly correlated with the fs laser dosage. This showed that the fs laser dosage should be carefully optimized if fs laser is to be employed in biomedical applications. In our experiments, the fs laser dosage of 55 mW/2 ms was able to contain the IHS within the safe range. Among the cells that were able to fully reseat their wounds,

over 90% had their holes resealed within 100 s. This suggested that the wound closure was a fairly fast process. For cells such as skeletal muscle cells and cardiac myocytes that often sustained repetitive plasma membrane disruptions during exercise, such capacity for wound closure was critical to tissue homeostasis and function sustainability.

General Difference Between the Oxidative Groups and the Control

The holes generated by fs laser in the oxidative groups were significantly bigger than those in the control. IHS in the oxidative groups were on the average beyond the formerly-defined safe range. With such bigger IHS, the resealing ratios of the three oxidative groups decreased accordingly. The resealing time for wound closure in the oxidative groups was much longer than that of the control. These results demonstrated that if the cells were already subjected to oxidative stress, their wound evolution after damage could be significantly affected. Oxidative stress compromised cellular resistance to laser photoporation and slowed their wound repair process. Wound repair of a single cell requires different cytoskeletal coordination, including the assembly of the actomyosin ring involving Rho family GTPases especially RhoA and Cdc42.⁵ Our group has recently discovered that H₂O₂ oxidative stress could threaten myoblast viability in a concentration-dependent manner. In response to H₂O₂ treatment, RhoA expression of myoblasts was down-regulated significantly.²⁵ Therefore, the assembly of the actomyosin ring in wound repair would probably be compromised for the low RhoA level after H₂O₂ treatment. The lower resealing ability of oxidative groups may result from the anomalous assembly of the actomyosin ring during the wound repair process with RhoA deficiency.

Chronic Oxidative Stress Caused Significantly More Damage than the Acute Oxidative Stress

The holes in 0.5 mM/24 h H₂O₂ group were significantly bigger than those of 0.5 and 2 mM/1 h groups. The resealing ratio of the 0.5 mM/24 h group was much lower than the control group and the other two short exposure H₂O₂ treatment groups. These results suggested that compared to the acute oxidative groups, the plasma membrane integrity might have been critically compromised by chronic H₂O₂ treatment before the fs laser damage. This observation was highly consistent with the earlier study of our group that cytoskeleton regulatory protein cofilin, serving to promote actin filament depolymerization, was

significantly higher after 0.5 mM/24 h H₂O₂ treatment, while its level showed a decreasing trend in the 0.5 and 2 mM/1 h treatment groups.²⁸ This up-regulation of cofilin likely compromised the cytoskeletal structure, which could lead to reduced resistance against biophysical damage and reduced capacity for plasma membrane repair. On the other hand, the down-regulation of cofilin in the 2 and 0.5 mM/1 h groups would suggest enhanced polymerizations of the cytoskeletal actins and thus strengthening of the cells.

According to Fig. 6b, the IHS of the three oxidative groups were generally in the interim range. The previous observation in the normal condition already showed that if the hole size was within the interim region, the resealing ratio of cell wounds fell below 50% (Fig. 7a). Now we compare the resealing ratios of all the cells with IHS in the interim range in the four different conditions (Fig. 9). Interestingly, for the two short-duration H₂O₂ treatment groups, the holes beyond the safe range showed a resealing ratio higher than the normal group after laser photoporation. This may suggest the possibility that the short exposure to oxidative stress promoted the intrinsic repair capacity of myoblasts against biophysical damage on the plasma membrane such as laser photoporation. This may result from the above-mentioned down-regulation of cofilin in the 2 and 0.5 mM/1 h groups. The apparent enhancement of repair capacity is also consistent with our study of the effects of chronic and short H₂O₂ exposures on the compressive damage thresholds of myoblasts in monolayer.²⁹ Cellular responses to oxidative stress were multi-faceted involving gene regulation, organelle function and cell behavior changes.⁹ It might be possible that these multi-facet responses may have certain indirect effects on the wound repair process. Such hypothesis should be carefully examined through further in-depth studies.

CONCLUSION

The hole-resealing process of myoblasts after fs laser photoporation was typical of cell wound evolution. Whether the wound could be fully closed was determined by the initial wound size. Cells tend to fully reseal their wounds when the wound size was within the safe range of 5 μm^2 . Oxidative stress compromised the plasma membrane integrity by inducing a bigger wound with the same laser dosage and slowing the subsequent wound closure process. Chronic oxidative stress could severely threaten the integrity of plasma membrane. Acute oxidative stress, on the other hand, may promote the resealing responses to the fs laser photoporation.

ACKNOWLEDGMENTS

The authors thank the Hong Kong Research Grants Council for its General Research Funding support for this work through the project Grant CUHK415413.

CONFLICT OF INTERESTS

The authors declare that they have no conflict of interests.

REFERENCES

- ¹Abreu-Blanco, M. T., J. M. Verboon, and S. M. Parkhurst. Cell wound repair in *Drosophila* occurs through three distinct phases of membrane and cytoskeletal remodeling. *J. Cell Biol.* 193(3):455–464, 2011.
- ²Abreu-Blanco, M. T., J. M. Verboon, and S. M. Parkhurst. Single cell wound repair: dealing with life's little traumas. *Bioarchitecture* 1(3):114–121, 2011.
- ³Antkowiak, M., M. L. Torres-Mapa, D. J. Stevenson, K. Dholakia, and F. J. Gunn-Moore. Femtosecond optical transfection of individual mammalian cells. *Nat. Protoc.* 8(6):1216–1233, 2013.
- ⁴Behl, C. Alzheimer's disease and oxidative stress: implications for novel therapeutic approaches. *Prog. Neurobiol.* 57(3):301–323, 1999.
- ⁵Benink, H. A., and W. M. Bement. Concentric zones of active RhoA and Cdc42 around single cell wounds. *J. Cell Biol.* 168(3):429–439, 2005.
- ⁶Cachofeiro, V., M. Goicochea, S. G. de Vinuesa, P. Oubiña, V. Lahera, and J. Luño. Oxidative stress and inflammation, a link between chronic kidney disease and cardiovascular disease. *Kidney Int.* 74:S4–S9, 2008.
- ⁷Cai, C., H. Masumiya, N. Weisleder, N. Matsuda, M. Nishi, M. Hwang, J. Ko, P. Lin, A. Thornton, X. Zhao, Z. Pan, S. Komazaki, M. Brotto, H. Takeshima, and J. Ma. MG53 nucleates assembly of cell membrane repair machinery. *Nat. Cell Biol.* 11(1):56–64, 2008.
- ⁸Celis, J. E. Microinjection of somatic cells with micropipettes: comparison with other transfer techniques. *Biochem. J.* 223(2):281, 1984.
- ⁹Davies, K. J. Oxidative stress, antioxidant defenses, and damage removal, repair, and replacement systems. *IUBMB Life* 50(4–5):279–289, 2000.
- ¹⁰Dean, D. A., D. Machado-Aranda, K. Blair-Parks, A. V. Yeldandi, and J. L. Young. Electroporation as a method for high-level nonviral gene transfer to the lung. *Gene Ther.* 10(18):1608–1615, 2003.
- ¹¹Gattass, R. R., and E. Mazur. Femtosecond laser micro-machining in transparent materials. *Nat. Photon.* 2(4):219–225, 2008.
- ¹²Halliwell, B. Oxidative stress and cancer: have we moved forward? *Biochem. J.* 401:1–11, 2007.
- ¹³Harding, H. P., Y. Zhang, H. Zeng, I. Novoa, P. D. Lu, M. Calfon, N. Sadri, C. Yun, B. Popko, R. Paules, D. F. Stojdl, J. C. Bell, T. Hettmann, J. M. Leiden, and D. Ron. An integrated stress response regulates amino acid metabolism and resistance to oxidative stress. *Mol. Cell* 11(3):619–633, 2003.

- ¹⁴Hu, Yaxin, Jennifer M. F. Wan, and Alfred C. H. Yu. Membrane perforation and recovery dynamics in microbubble-mediated sonoporation. *Ultrasound Med. Biol.* 39(12):2393–2405, 2013.
- ¹⁵Liu, J., T. N. Lewis, and M. R. Prausnitz. Non-invasive assessment and control of ultrasound-mediated membrane permeabilization. *Pharm. Res.* 15(6):918–924, 1998.
- ¹⁶Mandato, C. A., and W. M. Bement. Contraction and polymerization cooperate to assemble and close actomyosin rings around *Xenopus* oocyte wounds. *J. Cell Biol.* 154(4):785–798, 2001.
- ¹⁷McNeil, A. K., U. Rescher, V. Gerke, and P. L. McNeil. Requirement for annexin A1 in plasma membrane repair. *J. Biol. Chem.* 281(46):35202–35207, 2006.
- ¹⁸McNeil, P. L., and R. A. Steinhardt. Loss, restoration, and maintenance of plasma membrane integrity. *J. Cell Biol.* 137(1):1–4, 1997.
- ¹⁹McNeil, P. L., and R. A. Steinhardt. Plasma membrane disruption: repair, prevention, adaptation. *Annu. Rev. Cell Dev. Biol.* 19(1):697–731, 2003.
- ²⁰Pawley, J. *Handbook of Biological Confocal Microscopy*. Springer Science & Business Media, 2006.
- ²¹Powers, S. K., A. N. Kavazis, and J. M. McClung. Oxidative stress and disuse muscle atrophy. *J. Appl. Physiol.* 102(6):2389–2397, 2007.
- ²²Serpensu, E. H., K. Kinoshita, and T. Y. Tsong. Reversible and irreversible modification of erythrocyte membrane permeability by electric field. *Biochim. Biophys. Acta. (BBA)-Biomembr.* 812(3):779–785, 1985.
- ²³Siu, P. M., Y. Wang, and S. E. Alway. Apoptotic signaling induced by H₂O₂-mediated oxidative stress in differentiated C₂C₁₂ myotubes. *Life Sci.* 84(13):468–481, 2009.
- ²⁴Sonnemann, K. J., and W. M. Bement. Wound repair: toward understanding and integration of single-cell and multicellular wound responses. *Annu. Rev. Cell Dev. Biol.* 27:237–263, 2011.
- ²⁵Sun, S., S. Wong, A. Mak, and M. Cho. Impact of oxidative stress on cellular biomechanics and rho signaling in C₂C₁₂ myoblasts. *J. Biomech.* 47(15):3650–3656, 2014.
- ²⁶Tatham, P. E., and B. D. Gomperts. Rat mast cells degranulate in response to microinjection of guanine nucleotide. *J. Cell Sci.* 98(2):217–224, 1991.
- ²⁷Terasaki, M., K. Miyake, and P. L. McNeil. Large plasma membrane disruptions are rapidly resealed by Ca²⁺-dependent vesicle-vesicle fusion events. *J. Cell Biol.* 139(1):63–74, 1997.
- ²⁸Wong, S. W., S. Sun, M. Cho, K. K. Lee, and A. F. T. Mak. H₂O₂ exposure affects myotube stiffness and actin filament polymerization. *Ann. Biomed. Eng.* 1–11, 2014.
- ²⁹Yao, Y., Z. Xiao, S. W. Wong, Y. Hsu, T. Cheng, C. Chang, L. Bian, and A. Mak. The effects of oxidative stress on the compressive damage thresholds of C₂C₁₂ mouse myoblasts—implications for deep tissue injury. *Cells. Ann. Biomed. Eng.* 43(2):287–296, 2015.
- ³⁰Zhou, Y., J. Shi, J. Cui, and C. X. Deng. Effects of extracellular calcium on cell membrane resealing in sonoporation. *J Control Release* 126(1):34–43, 2008.